Amazonian terrestrial water balance inferred from satellite-derived water vapor isotopes

Mingjie Shi (mingjie.shi@pnnl.gov)
Pacific Northwest National Laboratory https://orcid.org/0000-0002-2469-4831

John Worden
JPL / Caltech https://orcid.org/0000-0003-0257-9549

Adriana Bailey
National Center for Atmospheric Research

David Noone
University of Auckland

Camille Risi
Laboratoire de Météorologie Dynamique

Rong Fu
JPL, University of California, Los Angeles

Sarah Worden
University of California, Los Angeles

Robert Herman
NASA Jet Propulsion Laboratory https://orcid.org/0000-0001-7063-6424

Vivienne Payne
Jet Propulsion Laboratory, California Institute of Technology https://orcid.org/0000-0002-9204-9703

Thomas Pagano
JPL/Caltech

Kevin Bowman
Jet Propulsion Laboratory

Alexis Bloom
Jet Propulsion Laboratory / California Institute for Technology

Sassan S Saatchi
University of California Los Angeles

Junjie Liu
Jet propulsion Laboratory, California Institute of Technology

Joshua Fisher
California Institute of Technology

Article

Keywords: Evapotranspiration, Precipitation, Water Stress, Variable Bias, Sensitivity Errors, Spatial Patterns

Posted Date: March 1st, 2021

DOI: https://doi.org/10.21203/rs.3.rs-237773/v1

Version of Record: A version of this preprint was published at Nature Communications on May 13th, 2022. See the published version at https://doi.org/10.1038/s41467-022-30317-4.

Article: Amazonian terrestrial water balance inferred from satellite-derived water vapor isotopes

Mingjie Shi[1],[2] John R. Worden[3], Adriana Bailey[4], David Noone[5], Camille Risi[6], Rong Fu[7], Sarah Worden[7], Robert Herman[3], Vivienne Payne[3], Thomas Pagano[3], Kevin Bowman[3], A. Anthony Bloom[3], Sassan Saatchi[3], Junjie Liu[3], and Joshua B. Fisher[3]

Corresponding Author: Mingjie Shi and John Worden

1. Joint Institute for Regional Earth System Science and Engineering and Department of Atmospheric and Oceanic Sciences, University of California, Los Angeles
2. Pacific Northwest National Laboratory
3. Jet propulsion Laboratory, California Institute of Technology
4. National Center for Atmospheric Research
5. University of Auckland
6. Laboratoire de Météorologie Dynamique
7. University of California, Los Angeles

Abstract

The evolution of the Amazon forest is tightly coupled to its terrestrial water balance (evapotranspiration minus precipitation, or ET-P), as an increase in ET-P reduces soil moisture, increasing water stress. However, large differences of ~50% between current monthly estimates of ET-P make it challenging to confidently quantify its spatio-temporal distribution and evolution. Here, we show that new satellite observations of the HDO/H_2O ratio of water vapor, spanning 2003 to 2020, constrain estimates of the Amazon water balance with monthly precision of ~20%. The HDO/H_2O ratio of water vapor is sensitive to the difference between ET and P, rather than to either flux alone, because lighter isotopes preferentially evaporate and heavier isotopes preferentially condense. Consequently, variable bias and sensitivity errors that result from combining different ET and precipitation products are minimized with this proxy. Our analysis demonstrates these data can quantify the spatial patterns of Amazon water balance from monthly to interannual time scales.

Introduction

The Amazon forests typically depends on rainfall exceeding ~2000 mm year^{-1} [1]. The rainfall in turn depends on advected oceanic moisture combined with the remaining from local evapotranspiration (ET) that can contribute up to 30–40% of the atmospheric moisture during the dry season[2,3] and is important for initiation of the seasonal monsoon over the Southern Amazon[4]. Characterizing the moisture balance of tropical ET and precipitation (or ET-P) and how it is controlled by climatic and anthropogenic forcings is therefore critical towards evaluating the fate of the tropical forest structure in the wet Amazon and the surrounding dry tropics. For example, an increase in ET-P directly over a moist tropical forest represents a local loss in water but is a source of rainfall for forests downwind[3], maintaining photosynthesis and forest growth in the dry tropics and the transition area between the moist and dry tropics[1,5]. However, quantifying this moisture balance, and how it changes, is challenging as it is the difference between two large fluxes, both with large uncertainties. These fluxes in turn are calculated through very different remote sensing or modeling approaches, leading to additional uncertainty in their difference because of seasonally dependent biases that depend on cloud and rain amount. For example, brightness temperature measurements and reanalysis are used to quantify ET[6–8], whereas radar and microwave measurements, or reanalysis, are used to quantify rainfall[9–11]. For these reasons, annual averaged Amazon ET estimates differ by approximately 30%[12]. Similarly, different rainfall estimates can vary by up to 10–20% in the Amazon for a yearly average[13] but up to 30 to 50% for monthly rainfall estimates[7,9,14]. Assuming that these variations are related to uncertainty and add in quadrature, this implies ~50% uncertainty in our knowledge of the monthly Amazon moisture balance, or ET-P.

Because ET-P over basin scales is equivalent to the change in water storage and river discharge, it can also be quantified using satellite gravity and river discharge measurements at the basin scale[15–17] (Methods). The errors in ET-P based on this approach are likely smaller at basin scales than those from visible or thermal remote sensing because the gravity data are precision limited and the errors in river discharge are thought to be 20%[15]; however, this error has not been thoroughly vetted using independent datasets, consequently, it could be much higher and/or vary by season[18]. Figure 1 shows the estimated ET-P over the Obidos basin (Basin 10 in Figure 1b) for a climatological average for the years between 2003 and 2015 using these different approaches for quantifying ET-P (Methods). We choose the Obidos basin for comparison as it is a relatively large basin in the Amazon (i.e., 74.9 Mha). Measurements in Obidos are taken of the water flow on a frequent basis[19] and are considered to be more accurate because the width of the river is relatively narrow. Figure 1a confirms that these different remote sensing approaches for quantifying ET-P have different seasonality, outside of their monthly variance over this time period (corresponding shading), although within the bounding error of ~50% discussed previously.

In this paper, we demonstrate that satellite measurements of the deuterium content of water vapor (or HDO/H_2O or D/H ratio) over the Amazon reflect the spatial, seasonal, and interannual variability of ET-P. Satellite observations of D/H ratio have been used for evaluating the primary moisture sources and dynamics affecting the tropical and sub-tropical water cycle [4,20–25]. The deuterium content of a measurement is traditionally given in parts per thousand relative to the deuterium content of ocean waters (or δD; Methods). Consequently, a value of zero means the measurement has the same deuterium content as the ocean and a value of -1000 permil means the measured air parcel has no deuterium. Processes that modify the deuterium content by preferentially selecting HDO over H_2O or vice versa are said to induce fractionation. The deuterium content of water vapor in the free troposphere over the tropical continents is primarily

modified by mixing of ET from nearby sources, transport of moisture from distant sources, and precipitation[21,25]. Rainfall depletes vapor of deuterium because isotopically heavier molecules preferentially condense; whereas mixing of evaporated or transpired water from the deuterium-rich ocean or land surface tends to increase the atmospheric δD. Furthermore, since transpiration and the complete evaporation of intercepted water from forest canopies produce little-to-no net fractionation, water vapor sourced from heavily vegetated areas is typically more enriched than water vapor originating from the ocean[21,25,26]. As discussed next, these data are sensitive to the difference between ET and precipitation and hence do not have uncertainties related to quantifying the difference between two large fluxes with very different seasonal biases and uncertainty characteristics.

Seasonality of Amazon ET-P using water vapor deuterium content

Precipitation and mixing processes change the atmospheric deuterium content and its bulk moisture content; thus, δD covaries, to zeroth order, with the water vapor amount (q) (Figure 2). However, the exact nature of this relationship depends on which process is dominant[21,27]. During a rainfall event, the deuterium content is gradually depleted, broadly following what is called a Rayleigh distillation, such that δD decreases proportionally with changes in ln(q)[28]. In contrast, when the free troposphere mixes with evapo-transpired water vapor in the boundary layer, HDO and H_2O concentrations vary linearly, such that δD changes proportionally with $1/q$[4]. The degree to which isotopic variations follow one or the other of these relationships is readily quantified by normalizing the δD to a reference water vapor concentration. Empirically, normalizing the isotopic composition to a reference value of 0.004 volume mixing ratio (VMR), typical of free-tropospheric concentrations (i.e., δD_004; Methods), serves as a linear proxy of the relative importance between evaporation and precipitation processes, as shown in Figure 2[29,30].

Figure 1 (purple line) shows the seasonality of δD_004 for the Obidos basin. These δD_004 data are generated from new Atmospheric Infrared Sounder (AIRS) measurements of the HDO/H_2O ratio of free-tropospheric water vapor[31,32], which are available from 2003 to 2020 (Methods). The AIRS deuterium measurements (Methods) and corresponding δD_004 estimates have a monthly uncertainty of ~4 permil with no observable changes in the calibration over this time period[33], making this record suitable for evaluating seasonal to decadal changes. Figure 1 shows that the seasonality of these AIRS estimates of δD_004 agrees with the terrestrial water storage (TWS) obtained from gravity measurements and river discharge-based ET-P estimate during the late rainy season in boreal spring and exhibits similar timing of peak values compared to the PT-JPL ET / satellite rainfall based ET-P estimate in the boreal fall late dry season, when we might expect uncertainties in the remote sensing estimate to be improved because of reduced rain and clouds.

Regressions based on observations and model simulations demonstrate more clearly the linearity between δD_004 and ET-P (Figure 3). For the observations, we use the sum of river discharge TWS change with time to represent ET-P (Eq. 1, Figure 3a). The model outputs are from an isotope-enabled version of the Community Atmosphere Model (iCAM5; Methods; Figure 3b)[34]. The comparisons are at a monthly time scale. Here, these model comparisons account for the vertical resolution and regularization used with the AIRS deuterium content retrievals[31]. We choose the three sub-regions shown in Figure 3 for comparison because advection from the Atlantic Ocean during the rainy season typically enters in the northeast of the basin and then circulates along the Andes towards the south[35]. Differences in the slope and offset between the three regions are likely due to different moisture sources, with the basins nearer to the ocean more

dependent on the less enriched ocean moisture source and the basins more inland having a larger ET signal with correspondingly higher deuterium content[25].

The iCAM5 estimates show much larger values of ET-P relative to observations. For example, the observations in Figure 3a show that ET-P is largely negative throughout the year over the wet tropics whereas the model has ET-P being positive for ~1/3 the year. These differences between observed and modeled ET-P will impart a slightly different range of values when scaling δD_004 to ET-P. Nevertheless, we expect iCAM5 to provide a realistic description of the large-scale circulation that affects the Amazon dry and rainy seasons. Consequently, while the slopes for model and data are different, highlighting the model bias in the composition of ET or advected water, they do change in the same manner between model and data; the region closest to the ocean has a larger slope and the regions away from the ocean have smaller slopes.

In addition to the variable slope and intercept across regions, we also expect a number of processes to contribute errors in projecting δD_004 to ET-P. These include variations in cloud and microphysical processes, changes in the depth of convection resulting in variations in moisture flux convergence (Figure 2), and bias in the AIRS sampling. The scatter in the deuterium content versus TWS/river discharge data are also likely driven by uncertainties in the river discharge data which are assumed to be 20% or larger. That said, uncertainties related to the deuterium content and gravity measurements are small relative to the other uncertainties mentioned since both are effectively precision limited, meaning that monthly averaging reduces their uncertainties[15,31,32,36]. These different effects are discussed in more detail in Methods.

We choose to quantify the uncertainties in projecting δD_004 to ET-P by regressing monthly (observed or simulated) δD_004 against ET-P and comparing the regression predictions with ET-P estimates from various combinations of observation-based products and iCAM outputs for the 14 distinct Amazon basins shown in Figure 1b (Tables S1-3). We quantify the precision through the comparison of iCAM because it describes the physics of the deuterium to ET-P relationship. As the variability of this relationship is driven by the model represented atmospheric dynamics, we expect this part of the error to be effectively random. The root mean square (RMS) differences between the iCAM5 δD_004 prediction and ET-P, for example, are found to range from ~33 to 58 mm month^{-1}, depending on the basin (Table S2). For every basin but number 14, these RMS differences are substantially smaller than the RMS differences between the AIRS δD_004-based prediction and the various observational estimates of ET-P based on other satellite or river discharge data. This finding indicates that uncertainties related to projecting δD_004 to ET-P are smaller than differences between current observational ET-P products. It also suggests that accuracy in the deuterium-based ET-P proxy will depend on the independent ET-P estimates used to calibrate δD_004, whether from remote sensing, re-analysis, or the gravity and river discharge estimates. The smallest RMS differences come from scaling the δD_004 using the TWS and river discharge estimates (Table S3)—an expected result because the GRACE data are precision limited, such that the differences shown in Table S3 are driven primarily by the accuracy of the river discharge data, a single source of error as opposed to multiple sources of error that arise from using the remote sensing of ET and rainfall products. The mean RMS difference for the comparisons to the TWS/discharge estimate is ~62 mm month^{-1}. Given that the yearly variability is ~250 mm month^{-1} (Figure 3), this indicates the monthly precision is ~20% and accuracy is ~25%. Based on this assessment, we choose to calibrate the AIRS δD_004 by regressing against the TWS/discharge estimates of ET-P for each individual basin (Table S1).

Spatial Variability of ET-P in Tropical South America

We next demonstrate how the deuterium proxy reflects the spatial variability of ET-P across the Amazon and to lesser extent the dry tropics of South America. After calibrating δD_004 using ET-P as calculated by the TWS and river discharge data (Table S1), the basin scale regression coefficients are then mapped to South America past the Amazon by using the regression coefficients from the basin that is closest to the grid cell. ET-P is calculated from these coefficients at a 2.5°×2.5° spatial resolution. Figure 4 shows ET-P based on this approach that spans the six months during the wet (January through June) and dry (July through December) seasons. These data confirm spatial gradients between the dry and wet tropics (demarcated as a white line in Figure 4) as shown with current remote-sensing based approaches[9]. We use the iCAM5 to quantify the uncertainty from this mapping approach and find that there is negligible contribution to the uncertainty budget in ET-P calculated for the Amazon but that ET-P estimates for regions outside the Amazon are likely biased low by about 40 mm month^{-1}. This bias is not just due to the extrapolation of results outside the Amazon but also because we find δD_004 is less correlated with ET-P in the dry tropics and more correlated with ET-P in the wet tropics (Methods), likely because of the strong influence of moisture advection from the wet tropics[4] as well as less local mixing between the surface and the free troposphere (Methods). Our motivation for showing the dry-tropical ET-P estimates is to demonstrate the feasibility and likely uncertainties for quantifying moisture balance in this region using the deuterium content data in subsequent studies.

Interannual Variability of Amazon ET-P

Our approach for quantifying ET-P can also be used for quantifying the interannual variability (IAV) of ET-P. Figure 5 shows a comparison between the de-seasonalized δD_004 and estimates of ET-P from the same data and model simulations shown in Figure 3. The model output (Figure 5b) demonstrates that we should expect the interannual variability of ET-P to co-vary with the δD_004 proxy. Similar behavior is shown with the comparisons between the IAV of the AIRS δD_004 and TWS/discharge estimates in Figure 5a, albeit with lower correlation than the model-based comparisons. In contrast to the seasonal comparisons shown in Table S3, the uncertainty in ET-P IAV, predicted using AIRS δD_004 and compared with the TWS/discharge IAV, is typically 20–50% better than uncertainties based on the other ET-P products shown in Table S4. However, we expect that the actual uncertainty is better than that reported in Table S4 because of poorly quantified uncertainties in the river data[15,37]. For example, the model-based estimates of ET-P IAV based on simulated dD_004 suggest an uncertainty of only ~20 mm month^{-1} (Methods; rightmost column of Table S5). The monthly uncertainty for δD _004 is ~4 per mil (Methods) which projects to an uncertainty of 8 mm month^{-1} given a typical slope between δD_004 and ET-P (Figure 5b). This suggests an uncertainty of ~22 mm month^{-1} for the IAV of ET-P. These uncertainties are more than sufficient for evaluating much of the interannual variability of ET-P demonstrated in Figure 5 because the maximum minus minimum values in the IAV is ~100 mm month^{-1}. Note that the slopes in Figure 5 are different than in Figure 3. However, if we first calibrate δD_004 to ET-P and then compare these de-seasonalized deuterium-based ET-P estimates to those from the de-seasonalized TWS/discharge estimates, the distributions follow a one-to-one line (Figure not shown), indicating that the distributions in Figures 5 and 3 are consistent.

Discussion and Implications

The evolution of forest structure is coupled to its water balance[38], since the latter determines available soil moisture and in turn the ability of a forest to uptake CO_2[39–41]. However, there are multiple possible outcomes for the evolution of the Amazon water balance in response to

climate change and anthropogenic impacts. For example, increasing CO_2 can improve photosynthetic efficiency, thus increasing water use efficiency and reducing transpiration[42]. However, increases in Amazon water vapor deficiency (VPD) can increase atmospheric demand of soil moisture, increasing ET if the forest is radiation water limited. In contrast, increasing VPD can also result from declining ET in water-limited areas[40], which may be driven by a decline in forest biomass. However, a concomitant increase in sensible heat can draw in remote moisture and hence mitigate the latent heat decline[25]. Indeed, during the 21st century, CO_2 has increased by nearly 10% while VPD in the southern Amazon has also increased[43] in the dry season. These observed drivers of ET and rainfall are changing even as remote suggest declines in precipitation and ET across the Amazon[44–46] of 5% or more. A stable, long-term record of Amazon water balance can help bound how short-term environmental changes (e.g. from ENSO) and long-term changes in environmental factors, such as CO_2 or VPD, determine water balance.

In this paper, we have demonstrated a new approach for quantifying the spatio-temporal variability of the Amazon water balance. These data have sufficiently small uncertainties to quantify ET-P from seasonal to inter-annual time scales. Longer term averages of these data have larger uncertainty reduction because the deuterium content data are effectively precision limited. A benefit of the AIRS instrument is its exceptional calibration stability, less than 0.06K or ~1/5000 change over the 20-year AIRS record[47], which can be extended further using observations from the NASA Cross-track Infrared Sounder (CRIS). Consequently, we anticipate that these data will open a new window into investigations on how climate and anthropogenic activities affect the moisture balance and its feedbacks on the carbon cycle in the Amazon. We also expect this same approach to be useful for the tropical forests in the Congo basin and S.E. Asia; however, additional analysis needs to be performed to calibrate this new deuterium based proxy to water balance over these regions.

Methods

Quantifying ET-P with observations from multiple observations

We use two independent approaches to quantify evapotranspiration minus precipitation (ET-P). One approach uses terrestrial water storage (TWS) retrievals from the Gravity Recovery and Climate Experiment (GRACE) and river discharge measurements over the Amazon by following the equation:

$$ET - P = -\frac{\Delta W}{\Delta t} - R \ , \quad (1)$$

where ET is evapotranspiration, P is precipitation, $\frac{\Delta W}{\Delta t}$ is TWS change with time, and R is runoff. Here, we use three GRACE TWS retrievals from the Center for Space Research (CSR), the GeoforschungsZentrum Potsdam (GFZ), and the Jet Propulsion Laboratory (JPL), and calculate the arithmetic mean of these GRACE TWS retrievals[48] to obtain $\frac{\Delta W}{\Delta t}$. Runoff data for each watershed are obtained from the Observation Service for the geodynamical, HYdrological and Biogeochemical control of erosion/alteration and material transport in the AMazon, Orinoco and Congo basins (SO-HYBAM) in-situ river-gauge discharge measurements spanning 2003–2015. Uncertainties are not provided with these estimates and could be as large as 20% or more for any given month[15] based on measurements taken over well-instrumented areas in the Western USA[18].

The value for R in Equation 1 is the net river discharge, that is the difference between the water leaving the basin and the water entering the basin [15,49].

A second approach is to quantify ET-P by using independent estimates for ET and for P. Here, we use four precipitation sources: the Global Precipitation Climatology Project (GPCP) at 2.5°×2.5° and monthly *spatiotemporal* resolution[50], the Tropical Rainfall Measuring Mission (TRMM) at 0.25°×0.25° and 3-hourly *spatiotemporal* resolution[11], the Precipitation Estimation from Remotely Sensed Information derived from Artificial Neural Networks (PERSIANN) at 0.25°×0.25° and daily spatio*temporal* resolution[51], and the Climate Research Unit (CRU) version 4 at 0.5°×0.5° and monthly *spatiotemporal* resolution[52]. Uncertainties between products can range from 30 to 100% at this resolution, depending on the amount of rain; we therefore take the mean of the four products and then calculate the monthly precipitation over the different basins shown in Figure 1. However, this approach does not reduce biases that are a result of variable sensitivity of the radar signal to rainfall amount[14].

We use a global ET estimate based on measurements from MODIS and MERRA, utilizing the ET algorithm of Priestley Taylor-Jet Propulsion Laboratory (PT-JPL), which also forms the core global ET retrieval for NASA's ECOSTRESS mission[53]. The uncertainty of this product is ~24 mm month^{-1} based on comparisons with surface site measurements across the tropics[6]; however, these uncertainties are not easily verified during the rainy season because of substantive cloud cover.

Use of Deuterium Content in Free-Tropospheric Water Vapor for Quantifying ET-P

In this study, we use atmospheric deuterium measurements from the Atmospheric Infrared Sounder (AIRS) and follow the method in Bailey *et al*. (2017) to quantify ET-P variations. The deuterium content of a measurement is expressed in parts per thousand relative to the deuterium content of ocean waters: $\delta D = 1000\left(\frac{R-R_{std}}{R_{std}}\right)$, where R is the ratio of the number of HDO molecules to the number of $H_2{}^{16}O$ molecules and R_{std} is the number of HDO molecules relative to number of $H_2{}^{16}O$ molecules in Vienna Standard Mean Ocean Water ($R_{std} = 3.11 \times 10^{-6}$).

As described extensively in previous research[21,27], if precipitation is the sole process modifying the moisture content of the atmosphere, the deuterium content follows a well-established distillation, in which δD decreases proportionally with changes in the natural logarithm of the water vapor volume mixing ratio (q). Assuming all condensate immediately precipitates, the change in δD with q follows the conventional Rayleigh distillation, illustrated by the red curve in Figure 2. In contrast, when ET is the sole process modifying the moisture content of the atmosphere, variations in δD with q can be modeled as a simple mixing process, in which water vapor in contact with the moisture source (i.e. the ocean or land surface) mixes with and moistens the free troposphere (blue and green curves). Numerous observational studies have shown that in most regions, the vast majority of isotopic observations fall somewhere between the Rayleigh and mixing curves, reflecting the significant role that both precipitation and ET play in regulating the atmosphere's moisture content[21,54–57].

The metric δD_004—first introduced in a study demonstrating that satellite measurements of water vapor isotopes can quantify ET-P[29]—quantifies the degree to which the atmosphere's hydrogen isotope ratio matches a precipitation-dominated or evaporation-dominated regime for a given water vapor concentration. Essentially, it is a measure of where the isotope ratio falls along the thin horizontal gray line in Figure 2.

To calculate δD_004 for each satellite observation, the observed HDO concentration profile is linearly regressed with the collocated H_2O concentration profile between pressure levels of approximately 325 hPa to 825 hPa—an altitude region where the AIRS' sensitivity to HDO is the largest[31]. The value of HDO for an H_2O volume mixing ratio of 0.004 is then found (herein HDO_004):

$$HDO_{004} = \beta_0 + \beta_1 \times 0.004 \quad (2)$$

where β_0 and β_1 are the intercept and slope relating the HDO and H_2O profiles at a given time and location. The HDO_004 concentration is then converted to delta notation following:

$$\delta D_{004} = \left(\frac{HDO_{004}}{0.004 \times R_{std}} - 1\right) \times 1000 \quad (3)$$

The more ET-dominated the environment, the higher its δD_004, while the more precipitation-dominated the environment, the lower its δD_004. However, the exact sensitivity of δD_004 to shifts in ET-P depends on the characteristics of the ET and precipitation processes in a particular region. The double-headed black arrow in Figure 2 represents the range of possible δD_004 values for an idealized tropical environment in which the precipitating atmosphere is perfectly pseudo-adiabatic (red curve), and the marine boundary layer (with lifting condensation level dew point and δD values arbitrarily set at 20°C and -72 permil, respectively) serves as the sole moisture source. However, the δD_004 range will expand or shrink depending on the characteristics of the moisture source, the efficiency of the precipitation, and the ability of convection to draw on remote moisture, as indicated by the other arrows in Figure 2. One factor that will extend the upper end of the δD_004 range, for example, is the relative contribution of transpiration to the total ET flux of the moisture source (green arrow). Because transpiration, on balance, produces almost no isotopic fractionation, the δD_004 response of tropical terrestrial environments to increasing ET-P can extend towards the green curve in Figure 2. In comparison, the low end of the δD_004 range tends to depend, instead, on the characteristics of precipitation. If, as is typical, the efficiency with which cloud water forms precipitation is less than 100%[58], isotopic depletion during precipitation will not be as great (pink arrow). Meanwhile, if rain evaporation occurs, reducing the efficiency with which precipitation reaches the surface, and if the evaporated fraction of the rain is very small, the isotopic depletion will be larger (purple arrow). It is noted that evaporation has a depleting effect on the vapor only if the rain evaporated fraction is very small (first order approximation in Worden et al. 2007). If, in contrast, the rain evaporated fraction is not small enough, rain evaporation has an enriching effect on the water vapor[59–61] (not shown). Microphysical processes within different regions of the atmospheric profile may thus have somewhat cancelling effects on the δD_004 sensitivity to ET-P. On the other hand, the reliance of convection on the convergence of remote moisture unambiguously extends the δD_004 range to lower values (orange arrow)[21]. Greater isotopic depletion is the result of convection incorporating ever-more rained out moisture at greater altitudes. Indeed, idealized modeling studies indicate that the degree to which convection relies on remote moisture (as opposed to local ET) is one of the most important factors determining tropical precipitation isotope ratios[62]. Consequently, one might expect that regions of the Amazon that lie farthest inland, whose local moisture is sourced from vegetated surfaces[3,4], and whose non-local moisture must travel a longer distance from the Atlantic coast, are more likely to exhibit a larger δD_004 sensitivity to shifts in ET-P. This suspicion is supported by the enhanced range in

precipitation isotope ratios found over inland areas of the Amazon Basin (compared to coastal areas) between the precipitation-dominated wet and evaporation-dominated dry seasons[63].

AIRS Measurements

The deuterium content of free tropospheric water vapor used in this analysis is derived from spectral radiances measured by the NASA AIRS satellite instrument[31]. The current record spans the time period from 2003 through 2019. The precision of a single observation of the integrated free-tropospheric deuterium content in the tropics is approximately 25 per mil[31]. Single-day averages over a ~2° latitude ×2° longitude have an uncertainty of ~8 per mil; the uncertainties in the data are somewhat correlated primarily due to the effects of temperature on the deuterium content retrieval[36]. However, further averaging is possible at monthly to seasonal time scales such that we expect the accuracy of averaged values at monthly time scales to be better than ~4 permil. This is because temperature acts in an almost random manner over monthly time scales. As discussed in the next methods section as well as in previous studies[25,64], the *a priori* constraint and averaging kernel must be applied to the atmosphere model fields before comparison to the data. However, we find there is no observable impact on our conclusions from this linear operation because the sensitivity of the AIRS measurement is sufficient to resolve the tropospheric deuterium content.

Quantifying the clear sky sampling bias of AIRS

The AIRS deuterium content retrievals shown here infer the HDO/H_2O ratio while also retrieving interfering effects such as cloud optical depth, atmospheric and surface temperature, and other trace gases that radiatively absorb and emit in the same 8 micron band. While cloud interference is therefore accounted for in the measurement, the data have a clear sky bias because the effect of clouds in the middle and upper troposphere is to reduce the sensitivity of the measurement, and low sensitivity measurements are not used in this analysis.

To quantify the bias towards low cloud conditions, we use large-eddy simulations (LES) enabled with isotopic physics[59,65]. We consider two simulations of radiative convective equilibrium: one without any large-scale vertical velocity and one with large-scale ascent with the large-scale vertical velocity profile peaking at 500hPa with a value of -60hPa d^{-1}. The simulations are run with a horizontal resolution of 750 m that allows us to explicitly simulate convective clouds and their associated updrafts and downdrafts[59]. Ten snapshots of the simulations, corresponding to the last 10 days of the simulation, are analyzed here.

To emulate what the AIRS satellite would sample if it was flying in the LES atmosphere, we randomly sample 49 locations in each of the 10 snapshots. We calculate the average cloud water path in a 15×15 km pixel around each of these locations, corresponding to the AIRS footprint. If the cloud water path is higher than a threshold, the pixel is discarded as cloudy. Otherwise, it is considered clear-sky, and we calculate the average humidity and δD profiles over the pixel. Finally, we average the humidity and δD profiles over all the clear-sky pixels. We compare these profiles to the domain-mean values (Figure S1 in Supplementary).

We find that the humidity and δD profiles averaged over clear-sky pixels differ from those in the domain-mean by less than a few percentages and permil, respectively. This is the case even in the strong convective conditions that are simulated in the case with large-scale ascent. When looking at δD_004, the difference is even smaller: the difference is only 0.04 permil and 0.7 permil for the case without and with large-scale ascent, respectively. Therefore, we can safely conclude that the effect of the clear-sky sampling bias can be neglected, likely because the humidity and δD

vary at spatial horizontal scales that are much larger than the size of a cloud, due to very strong mixing between the clouds and their environment[66].

Model description and model-based simulations of deuterium content

In this study, we use the isotope-enabled Community Atmospheric Model Version 5 (herein iCAM), which includes isotopic physics routines, and is able to simulate the modern distribution of water isotopologues in vapor and precipitation[34]. Here, we use the sea surface temperature (SST) during 2002–2017 to drive iCAM at the 1.9° latitude ×2.5° longitude spatial resolution, and we archive the monthly global output.

For simulating the AIRS δD_004 in Figures 3 and 5, we apply the mean AIRS averaging kernel, and *a priori* constraint for the corresponding time periods, latitude, and longitude is applied to the HDO/H_2O ratio from the model to account for the regularization and vertical resolution of the AIRS instrument. However, we find that because the AIRS sensitivity is sufficient to resolve the free-troposphere, the application of the averaging kernel and *a priori* do not substantively change the vertical profile of δD[31].

Quantifying the spatial representativeness of the deuterium-based ET-P proxy beyond the wet Amazon

One way to look at how well δD_004 can quantify ET-P in the tropics is to quantify the correlations between δD_004 and ET-P in one small region (e.g., a 2°×2° grid cell) and between δD_004 in this region and ET-P in other regions. This allows us to determine if the observed δD_004 is representative of ET-P over that region and also to provide a measure of the spatial resolution of the ET-P estimate. We use δD_004 from AIRS and ET-P obtained from PT-JPL ET and GPCP precipitation as well as the δD_004 and ET-P from iCAM. Here, we choose three ~2°×2° regions in Basins 10, 12 (in Venezuela), and 6, representing relatively wet (Basins 10 and 12) and dry (Basin 6) areas in Amazonia. Figures S2–S4 (Supplementary) shows that in general the highest correlations between δD_004 and ET-P from remote sensing are in the wet tropics, whereas δD_004 in the dry tropics is mostly correlated with ET-P in the wet tropics (Figure S4), likely because of the non-local dependence of free-tropospheric air in the dry tropics. The correlations become negative in Northern Hemisphere (Figures S2 and S4). Observations and iCAM suggest the same conclusion, even though there are spatial pattern differences between the models and observations. We will investigate in a subsequent manuscript if use of deuterium in the boundary layer better represents nearby variations in ET-P in the dry tropics, which we might expect as previous studies suggest a strong relationship of continental recycling with near-surface deuterium content of water vapor[25]. For these reasons we suggest caution in interpreting variations in δD_004 with respect to ET-P in the mountain regions or in the dry tropics. The correlations indicate that this new deuterium proxy can at least resolve ET-P in the northern part of S. America (e.g., the Venezuela/Guyana region; Figure S3) as well as the Eastern, Western, and S. Western part of the Amazon as indicated by the skill in which the deuterium proxy can fit ET-P in these regions and resolve the different slopes. The deuterium proxy can quantify ET-P in the south but additional analysis is needed to determine if this proxy has more information content than current approaches. A more refined spatial resolution estimate could be quantified using the averaging kernel matrix[67], for example, but this is beyond the scope of this paper.

Quantifying the uncertainty of ET-P with remote sensing observations and models

We quantify the uncertainty in the seasonal and interannual variability of the deuterium based ET-P estimates through comparison with different remote sensing products, re-analysis, the TWS and discharge data, and the iCAM. The different precipitation products are discussed in the previous section of Methods. In addition to PT-JPL ET, we also use the latent heat flux (J m^{-2} day^{-1}) from the fifth generation ECMWF re-analysis (ERA5), and convert the latent heat to ET (mm $month^{-1}$; herein ERAET). Thus, we have nine groups of ET-P based on different combinations (Table 3), and calculate the error in fit between these nine ET-P and ET-P estimation with δD_004. In addition, the error in fit between ET-P estimation from δD_004 and ET-P are calculated with iCAM output (Table S5). These different comparisons are used to evaluate the uncertainties in the seasonality and interannual variability (IAV) of the δD_004 based ET-P estimates.

Acknowledgements
This research was carried out at the Jet Propulsion Laboratory, California Institute of Technology, under a contract with the National Aeronautics and Space Administration. JBF was supported in part by NASA programs: ECOSTRESS and SUSMAP. Part of this material is based upon work supported by the National Center for Atmospheric Research, which is a major facility sponsored by the National Science Foundation under Cooperative Agreement No. 1852977. MS was partly supported by the U.S. Department of Energy Office of Science Biological and Environmental Research as part of the Terrestrial Ecosystem Science Program through the Next-Generation Ecosystem Experiments (NGEE) Tropics project. PNNL is operated by Battelle Memorial Institute for the U.S. DOE under contract DE-AC05-76RLO1830.

Data availability
All data needed to evaluate the conclusions in the paper are present in the paper and/or the Supplementary Information. Additional data related to this paper can be requested from the corresponding authors.

Author contributions
John Worden led and designed the analysis approach. Mingjie Shi performed the analysis. Adriana Bailey provided interpretation of the deuterium-based ET-P proxy. Mingjie Shi, John Worden, Adriana Bailey, and Joshua Fisher wrote the paper. David Noone, Camille Risi, Rong Fu, and Sarah Worden supported the analysis through modeling studies and interpretation of re-analysis. Robert Herman, Vivienne Payne and David Noone supported calibration and validation of the satellite deuterium data. Thomas Pagano supported interpretation of the AIRS instrument calibration. Kevin Bowman, Anthony Bloom, Sassan Saatchi, Michael Keller, Junjie Liu and Joshua Fisher provided ET estimates and supported interpretation.

References

1. Guan, K. *et al.* Photosynthetic seasonality of global tropical forests constrained by hydroclimate. *Nature Geoscience* **8**, (2015).
2. Gat, J. R. & Matsui, E. Atmospheric water balance in the Amazon Basin: an isotopic evapotranspiration model. *Journal of Geophysical Research* **96**, (1991).
3. Staal, A. *et al.* Forest-rainfall cascades buffer against drought across the Amazon. *Nature Climate Change* **8**, (2018).
4. Wright, J. S. *et al.* Rainforest-initiated wet season onset over the southern Amazon. *Proceedings of the National Academy of Sciences of the United States of America* **114**, (2017).
5. Green, J. K. *et al.* Regionally strong feedbacks between the atmosphere and terrestrial biosphere. *Nature Geoscience* **10**, (2017).
6. Fisher, J. B. *et al.* The land-atmosphere water flux in the tropics. *Global Change Biology* **15**, (2009).
7. Fisher, J. B. *et al.* The future of evapotranspiration: Global requirements for ecosystem functioning, carbon and climate feedbacks, agricultural management, and water resources. *Water Resources Research* vol. 53 (2017).
8. Fisher, J. B. *et al.* ECOSTRESS: NASA's Next Generation Mission to Measure Evapotranspiration From the International Space Station. *Water Resources Research* **56**, (2020).
9. Munier, S. & Aires, F. A new global method of satellite dataset merging and quality characterization constrained by the terrestrial water budget. *Remote Sensing of Environment* **205**, (2018).
10. Bookhagen, B. & Burbank, D. W. Toward a complete Himalayan hydrological budget: Spatiotemporal distribution of snowmelt and rainfall and their impact on river discharge. *Journal of Geophysical Research: Earth Surface* **115**, (2010).
11. Huffman, G. J. *et al.* The TRMM Multisatellite Precipitation Analysis (TMPA): Quasi-global, multiyear, combined-sensor precipitation estimates at fine scales. *Journal of Hydrometeorology* **8**, (2007).
12. Wu, J. *et al.* The reliability of global remote sensing evapotranspiration products over Amazon. *Remote Sensing* **12**, (2020).
13. Fekete, B. M., Vörösmarty, C. J., Roads, J. O. & Willmott, C. J. Uncertainties in precipitation and their impacts on runoff estimates. *Journal of Climate* **17**, (2004).
14. Rauniyar, S. P., Protat, A. & Kanamori, H. Uncertainties in TRMM-Era multisatellite-based tropical rainfall estimates over the Maritime Continent. *Earth and Space Science* **4**, (2017).
15. Rodell, M. *et al.* Basin scale estimates of evapotranspiration using GRACE and other observations. *Geophysical Research Letters* **31**, (2004).
16. Swenson, S. & Wahr, J. Estimating large-scale precipitation minus evapotranspiration from GRACE satellite gravity measurements. *Journal of Hydrometeorology* **7**, (2006).
17. Maeda, E. E. *et al.* Evapotranspiration seasonality across the Amazon Basin. *Earth System Dynamics* **8**, (2017).
18. David, C. H. *et al.* Analytical Propagation of Runoff Uncertainty Into Discharge Uncertainty Through a Large River Network. *Geophysical Research Letters* **46**, (2019).

19. Callede, J., Guyot, J. L., Ronchail, J., Molinier, M. & de Oliveira, E. The River Amazon at Óbidos (Brazil): Statistical studies of the discharges and water balance. *Hydrological Sciences Journal* **47**, (2002).
20. Worden, J. *et al.* Tropospheric Emission Spectrometer observations of the tropospheric HDO/H2O ratio: Estimation approach and characterization. *Journal of Geophysical Research Atmospheres* **111**, (2006).
21. Worden, J. *et al.* Importance of rain evaporation and continental convection in the tropical water cycle. *Nature* **445**, (2007).
22. Frankenberg, C. *et al.* Dynamic processes governing lower-tropospheric HDO/H2O Ratios as Observed from Space and Ground. *Science* **325**, (2009).
23. Good, S. P., Mallia, D. v., Lin, J. C. & Bowen, G. J. Stable isotope analysis of precipitation samples obtained via crowdsourcing reveals the spatiotemporal evolution of superstorm sandy. *PLoS ONE* **9**, (2014).
24. Brown, D., Worden, J. & Noone, D. Characteristics of tropical and subtropical atmospheric moistening derived from Lagrangian mass balance constrained by measurements of HDO and H 2O. *Journal of Geophysical Research Atmospheres* **118**, (2013).
25. Risi, C., Noone, D., Frankenberg, C. & Worden, J. Role of continental recycling in intraseasonal variations of continental moisture as deduced from model simulations and water vapor isotopic measurements. *Water Resources Research* **49**, (2013).
26. Galewsky, J. & Samuels-Crow, K. Water vapor isotopic composition of a stratospheric air intrusion: Measurements from the Chajnantor Plateau, Chile. *Journal of Geophysical Research: Atmospheres* **119**, (2014).
27. Noone, D. Pairing measurements of the water vapor isotope ratio with humidity to deduce atmospheric moistening and dehydration in the tropical midtroposphere. *Journal of Climate* **25**, (2012).
28. Galewsky, J. Constraining supersaturation and transport processes in a south American cold-air outbreak using stable isotopologues of water vapor. *Journal of the Atmospheric Sciences* **72**, (2015).
29. Bailey, A., Blossey, P. N., Noone, D., Nusbaumer, J. & Wood, R. Detecting shifts in tropical moisture imbalances with satellite-derived isotope ratios in water vapor. *Journal of Geophysical Research* **122**, (2017).
30. Dee, S. G. *et al.* Tracking the Strength of the Walker Circulation With Stable Isotopes in Water Vapor. *Journal of Geophysical Research: Atmospheres* **123**, (2018).
31. Worden, J. R. *et al.* Characterization and evaluation of AIRS-based estimates of the deuterium content of water vapor. *Atmospheric Measurement Techniques* **12**, (2019).
32. Herman, R. L. *et al.* Comparison of optimal estimation HDO⁄H₂O retrievals from AIRS with ORACLES measurements. *Atmospheric Measurement Techniques* **13**, (2020).
33. Aumann, H. H., Broberg, S., Manning, E. & Pagano, T. Radiometric Stability Validation of 17 Years of AIRS Data Using Sea Surface Temperatures. *Geophysical Research Letters* **46**, (2019).
34. Nusbaumer, J., Wong, T. E., Bardeen, C. & Noone, D. Evaluating hydrological processes in the Community Atmosphere Model Version 5 (CAM5) using stable isotope ratios of water. *Journal of Advances in Modeling Earth Systems* **9**, (2017).

35. Fu, R., Zhu, B. & Dickinson, R. E. How Do Atmosphere and Land Surface Influence Seasonal Changes of Convection in the Tropical Amazon? *Journal of Climate* **12**, (1999).
36. Kulawik, S. W. J. P. V. Evaluation of single-footprint AIRS CH4 Profile Retrieval Uncertainties Using Aircraft Profile Measurements. *Atmos. Meas. Tech. Discuss* (2020).
37. Azarderakhsh, M., Rossow, W. B., Papa, F., Norouzi, H. & Khanbilvardi, R. Diagnosing water variations within the Amazon basin using satellite data. *Journal of Geophysical Research Atmospheres* **116**, (2011).
38. McIntyre, P. J. *et al.* Twentieth-century shifts in forest structure in California: Denser forests, smaller trees, and increased dominance of oaks. *Proceedings of the National Academy of Sciences of the United States of America* vol. 112 (2015).
39. Fung, I. Y., Doney, S. C., Lindsay, K. & John, J. Evolution of carbon sinks in a changing climate. *Proceedings of the National Academy of Sciences of the United States of America* **102**, (2005).
40. Gentine, P. *et al.* Coupling between the terrestrial carbon and water cycles - A review. *Environmental Research Letters* vol. 14 (2019).
41. Green, J. K. *et al.* Large influence of soil moisture on long-term terrestrial carbon uptake. *Nature* **565**, (2019).
42. Eamus, D. The interaction of rising CO2 and temperatures with water use efficiency. *Plant, Cell & Environment* **14**, (1991).
43. Armineh Barkhordarian, K. B. N. C. J. J. J. L. Emergent constraints on climate—carbon cycle feedbacks from tropical atmospheric aridity. *Research Square*.
44. Swann, A. L. S. & Koven, C. D. A direct estimate of the seasonal cycle of evapotranspiration over the Amazon Basin. *Journal of Hydrometeorology* **18**, (2017).
45. Rodell, M. *et al.* Emerging trends in global freshwater availability. *Nature* **557**, (2018).
46. John Worden, S. S. M. K. A. B. et al. Satellite Observations of the Tropical Terrestrial Carbon Balance and Interactions with the Water Cycle During the 21st Century. *Review of Geophysics* (2021) doi:10.1029/2020RG000711.
47. Aumann, H. H., Broberg, S. E., Manning, E. M., Pagano, T. S. & Wilson, R. C. Evaluating the absolute calibration accuracy and stability of AIRS using the CMC SST. *Remote Sensing* vol. 12 (2020).
48. Sakumura, C., Bettadpur, S. & Bruinsma, S. Ensemble prediction and intercomparison analysis of GRACE time-variable gravity field models. *Geophysical Research Letters* **41**, (2014).
49. Shi, M. *et al.* The 2005 Amazon Drought Legacy Effect Delayed the 2006 Wet Season Onset. *Geophysical Research Letters* **46**, (2019).
50. Adler, R. F. *et al.* The Global Precipitation Climatology Project (GPCP) monthly analysis (New Version 2.3) and a review of 2017 global precipitation. *Atmosphere* **9**, (2018).
51. Ashouri, H. *et al.* PERSIANN-CDR: Daily precipitation climate data record from multisatellite observations for hydrological and climate studies. *Bulletin of the American Meteorological Society* **96**, (2015).
52. New, M., Hulme, M. & Jones, P. Representing twentieth-century space-time climate variability. Part II: Development of 1901-96 monthly grids of terrestrial surface climate. *Journal of Climate* **13**, (2000).

53. Fisher, J. B., Tu, K. P. & Baldocchi, D. D. Global estimates of the land-atmosphere water flux based on monthly AVHRR and ISLSCP-II data, validated at 16 FLUXNET sites. *Remote Sensing of Environment* **112**, (2008).
54. Lee, J. E. *et al.* Forest productivity and water stress in Amazonia: Observations from GOSAT chlorophyll fluorescence. *Tohoku Journal of Experimental Medicine* **230**, (2013).
55. Noone, D. *et al.* Properties of air mass mixing and humidity in the subtropics from measurements of the D/H isotope ratio of water vapor at the Mauna Loa Observatory. *Journal of Geophysical Research Atmospheres* **116**, (2011).
56. Bailey, A., Nusbaumer, J. & Noone, D. Precipitation efficiency derived from isotope ratios in water vapor distinguishes dynamical and microphysical influences on subtropical atmospheric constituents. *Journal of Geophysical Research* **120**, (2015).
57. González, Y. *et al.* Detecting moisture transport pathways to the subtropical North Atlantic free troposphere using paired H₂O-δ D in situ measurements. *Atmospheric Chemistry and Physics Discussions* **15**, (2015).
58. Cronin, T. W. & Wing, A. A. Clouds, Circulation, and Climate Sensitivity in a Radiative-Convective Equilibrium Channel Model. *Journal of Advances in Modeling Earth Systems* **9**, (2017).
59. Risi, C., Muller, C. & Blossey, P. What Controls the Water Vapor Isotopic Composition Near the Surface of Tropical Oceans? Results From an Analytical Model Constrained by Large-Eddy Simulations. *Journal of Advances in Modeling Earth Systems* **12**, (2020).
60. Risi, C. *et al.* Understanding the Sahelian water budget through the isotopic composition of water vapor and precipitation. *Journal of Geophysical Research Atmospheres* **115**, (2010).
61. Tremoy, G. *et al.* Clustering mesoscale convective systems with laser-based water vapor δ18O monitoring in niamey (Niger). *Journal of Geophysical Research* **119**, (2014).
62. Moore, M., Blossey, P. N., Muhlbauer, A. & Kuang, Z. Microphysical controls on the isotopic composition of wintertime orographic precipitation. *Journal of Geophysical Research* **121**, (2016).
63. Salati, E. & Vose, P. B. Amazon Basin: A system in equilibrium. *Science* **225**, (1984).
64. Sutanto, S. J. *et al.* Global-scale remote sensing of water isotopologues in the troposphere: Representation of first-order isotope effects. *Atmospheric Measurement Techniques* **8**, (2015).
65. Khairoutdinov, M. F. & Randall, D. A. Cloud resolving modeling of the ARM summer 1997 IOP: Model formulation, results, uncertainties, and sensitivities. *Journal of the Atmospheric Sciences* **60**, (2003).
66. Kuang, Z. & Bretherton, C. S. A mass-flux scheme view of a high-resolution simulation of a transition from shallow to deep cumulus convection. *Journal of the Atmospheric Sciences* **63**, (2006).
67. Rodgers, C. D. & Connor, B. J. Intercomparison of remote sounding instruments. *Journal of Geophysical Research: Atmospheres* **108**, (2003).

Figures

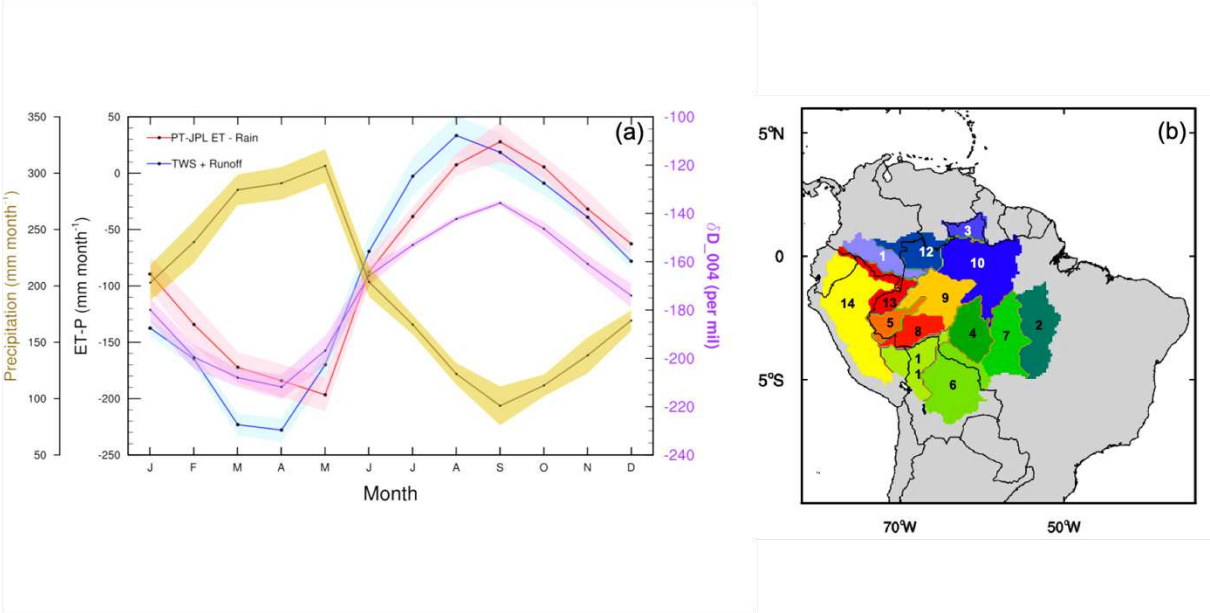

Figure 1. (a) The seasonality of evapotranspiration minus precipitation (ET-P) and δD_004 in the Obidos Basin (Basin 10) and (b) the watershed distribution map over Amazon. Estimates of ET-P are based on PT-JPL ET and the mean of four precipitation products: TRMM, GPCP, PERSIANN, and CRU. Terrestrial water storage (TWS) is from GRACE, runoff is from Amazon watershed measurements, and δD_004 is from AIRS. The error bars are calculated with the interannual variability of the products.

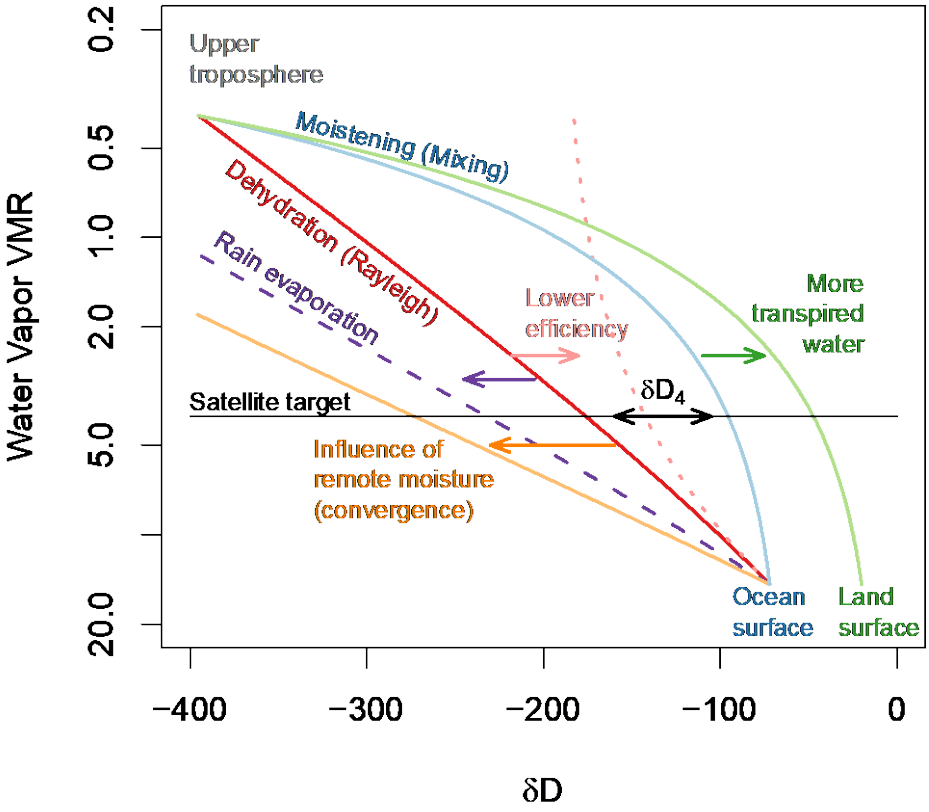

Figure 2. The processes influencing δD_004 variability, shown on a plot of water vapor volume mixing ratio (y-axis) versus δD (x-axis). For a constant water vapor volume mixing ratio (4 mmol mol^{-1}, flat gray line), variations in the hydrogen isotope ratio (δD_004, shortened in the Figure to (δD_4) represent the shifting importance of precipitation vs. evapotranspiration (ET-P). The precise scaling of δD_004 to ET-P will be modified by the efficiency of rainout and by the source of moisture to the atmosphere. For example, the two-sided black arrow shows the expected range of δD_004 if oceanic evaporation is the sole source of moisture to the atmosphere (blue line) and condensate formed during convection is immediately removed from the atmosphere by precipitation (red line). The intersection of the blue and red lines with the thin gray line explicitly shows the expected δD_004 values if P=0 or ET=0, respectively. As the contribution of transpiration to atmospheric moistening increases (green line), the δD_004 range will extend to the right, causing the expected δD_004 value to be higher when P=0. Contrastingly, as either rain evaporation (purple dashed line) or remote moisture convergence becomes important (orange line), the δD_004 range will extend to lower isotope ratios, causing the expected δD_004 value to be lower when ET=0. Decreasing the efficiency with which condensate forms precipitation (pink dotted line) will, in comparison, increase the expected δD_004 value when ET=0, limiting the expected δD_004 range for a given set of ET-P states.

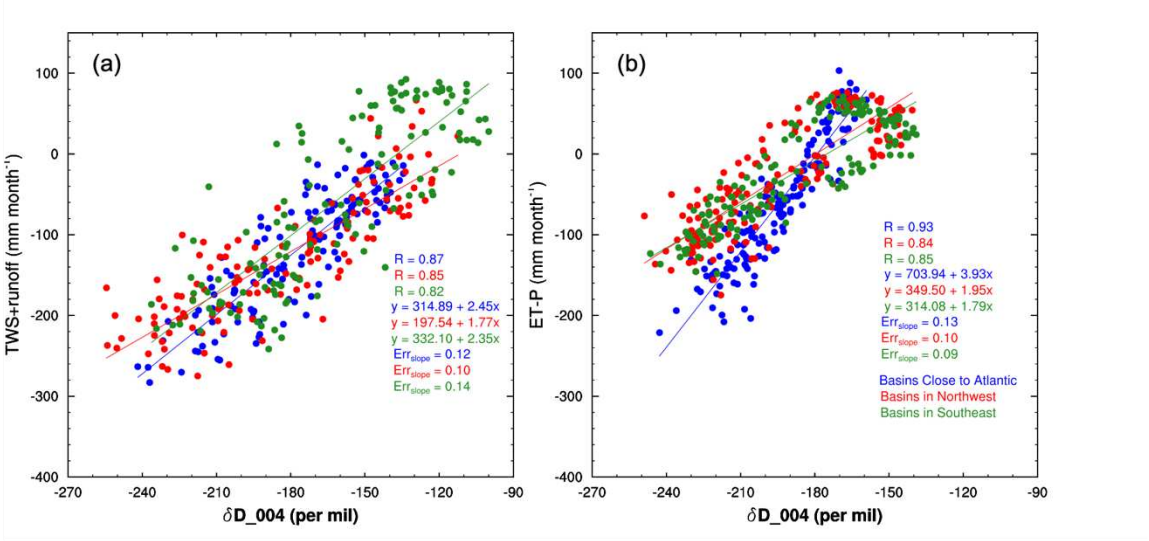

Figure 3. (a) Regressions of TWS/discharge estimated ET-P on AIRS δD_004 and (b) regressions of ET-P on δD_004 in ICAM. Basins close to the Atlantic are Basins 1, 3, 10, and 12; basins in the Northwest are basins 5, 8, 9,13, and 14; the rest of the basins are in the Southeast. Here, the basins close to the Atlantic have a higher slope than the others, according to both the observations and model, indicating a different moisture source.

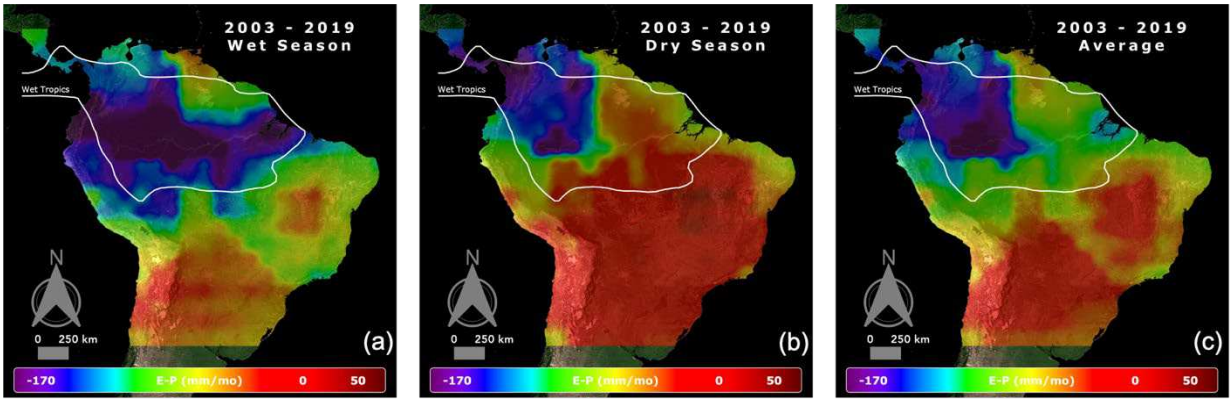

Figure 4. ET-P derived from δD_004 for the wet season (Jan-Jun), the dry season (Jul-Dec), and the annual average. The solid white line indicates the approximate boundary of the wet tropics, with rainfall inside the white line exceeding 160 mm month^{-1} on average over the year.

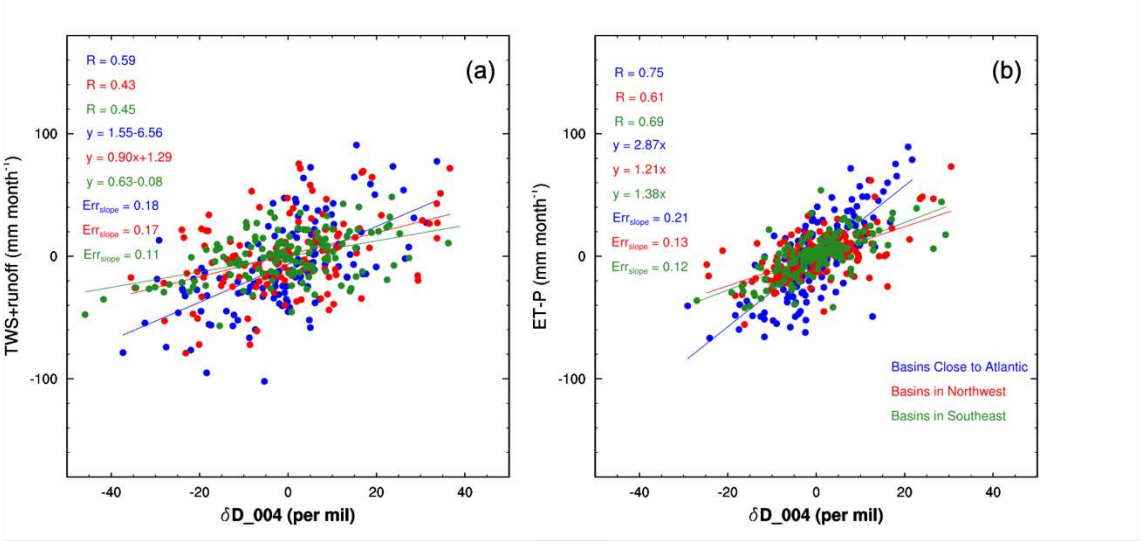

Figure 5. Similar to Figure 3, this figure shows IAV (a) regressions of TWS/discharge estimated ET-P on AIRS δD_004 and (b) regressions of ET-P on δD_004 in iCAM. Here, all the time series from observations and the model are de-seasonalized.

Figures

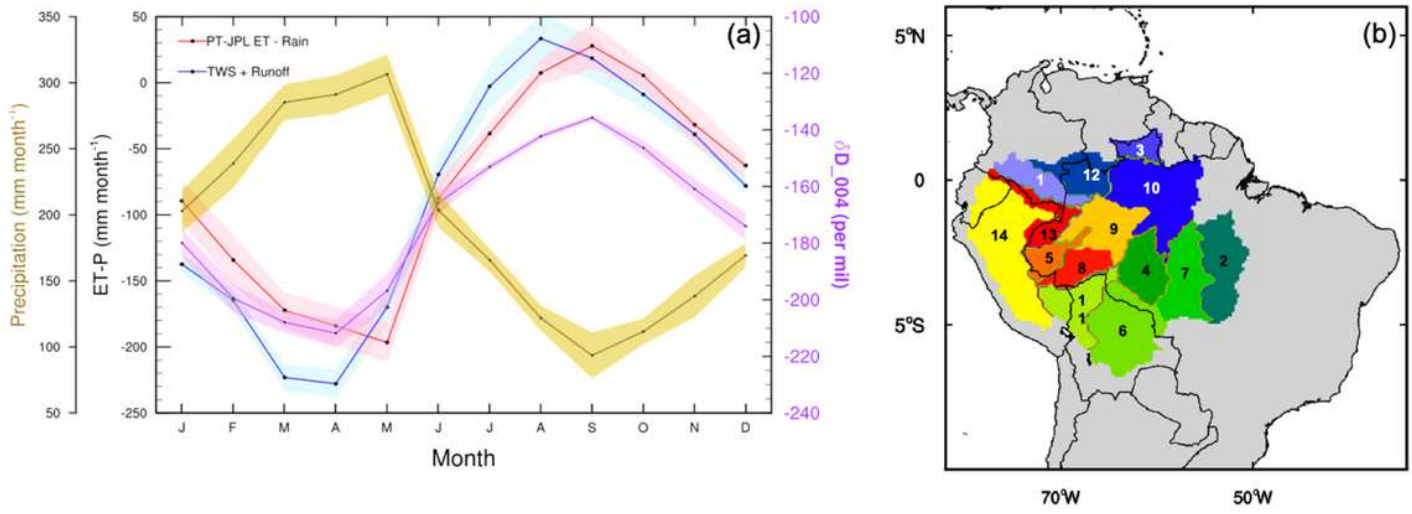

Figure 1

(a) The seasonality of evapotranspiration minus precipitation (ET-P) and δD_004 in the Obidos Basin (Basin 10) and (b) the watershed distribution map over Amazon. Estimates of ET-P are based on PT-JPL ET and the mean of four precipitation products: TRMM, GPCP, PERSIANN, and CRU. Terrestrial water storage (TWS) is from GRACE, runoff is from Amazon watershed measurements, and δD_004 is from AIRS. The error bars are calculated with the interannual variability of the products.

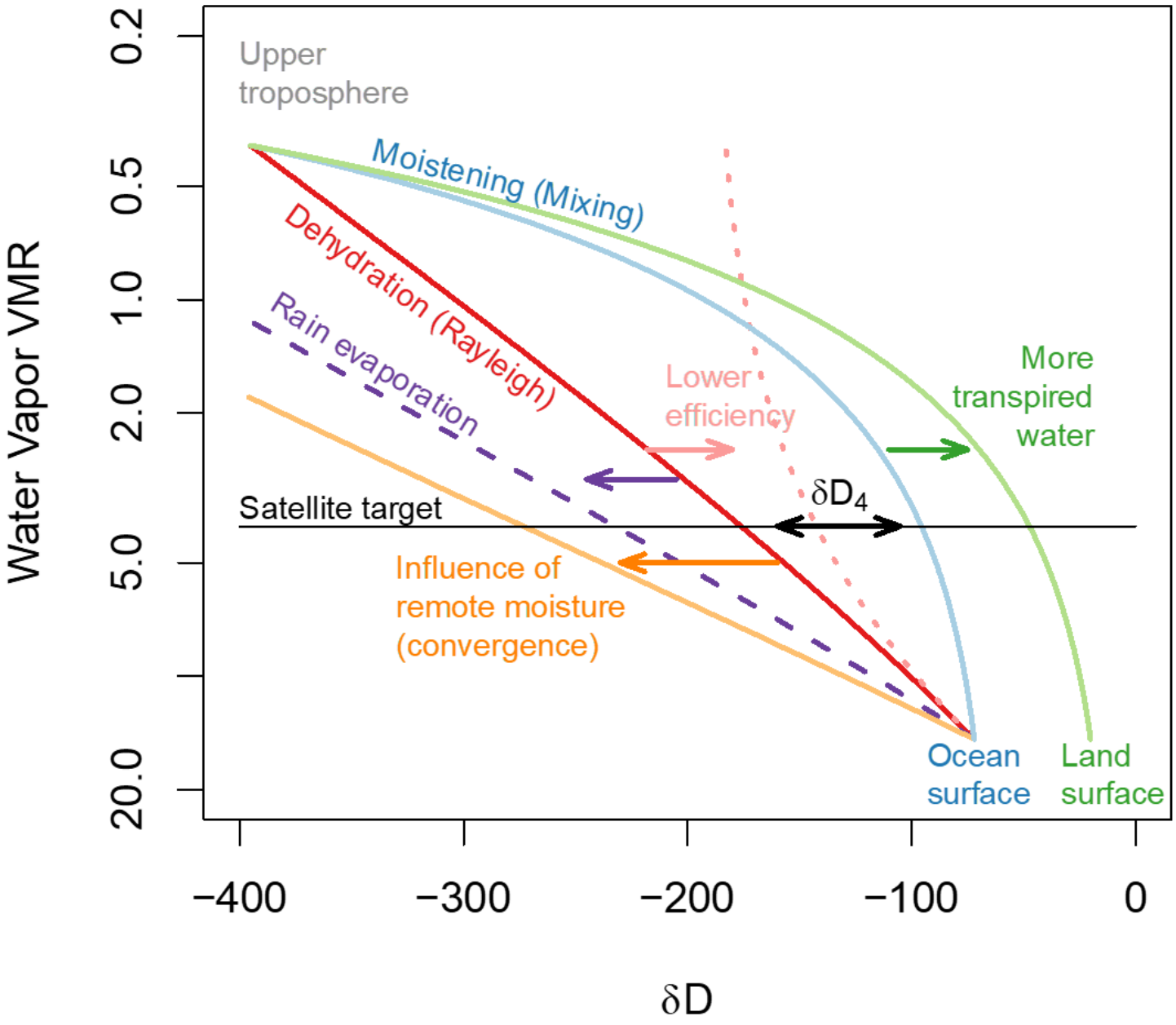

Figure 2

The processes influencing D_004 variability, shown on a plot of water vapor volume mixing ratio (y-axis) versus δD (x-axis). For a constant water vapor volume mixing ratio (4 mmol mol-1, flat gray line), variations in the hydrogen isotope ratio (δD_004, shortened in the Figure to (δD4) represent the shifting importance of precipitation vs. evapotranspiration (ET-P). The precise scaling of δD_004 to ET-P will be modified by the efficiency of rainout and by the source of moisture to the atmosphere. For example, the two-sided black arrow shows the expected range of δD_004 if oceanic evaporation is the sole source of moisture to the atmosphere (blue line) and condensate formed during convection is immediately removed from the atmosphere by precipitation (red line). The intersection of the blue and red lines with the thin gray line explicitly shows the expected δD_004 values if P=0 or ET=0, respectively. As the contribution of transpiration to atmospheric moistening increases (green line), the δD_004 range will extend to the right,

causing the expected δD_004 value to be higher when P=0. Contrastingly, as either rain evaporation (purple dashed line) or remote moisture convergence becomes important (orange line), the δD_004 range will extend to lower isotope ratios, causing the expected δD_004 value to be lower when ET=0. Decreasing the efficiency with which condensate forms precipitation (pink dotted line) will, in comparison, increase the expected δD_004 value when ET=0, limiting the expected δD_004 range for a given set of ET-P states.

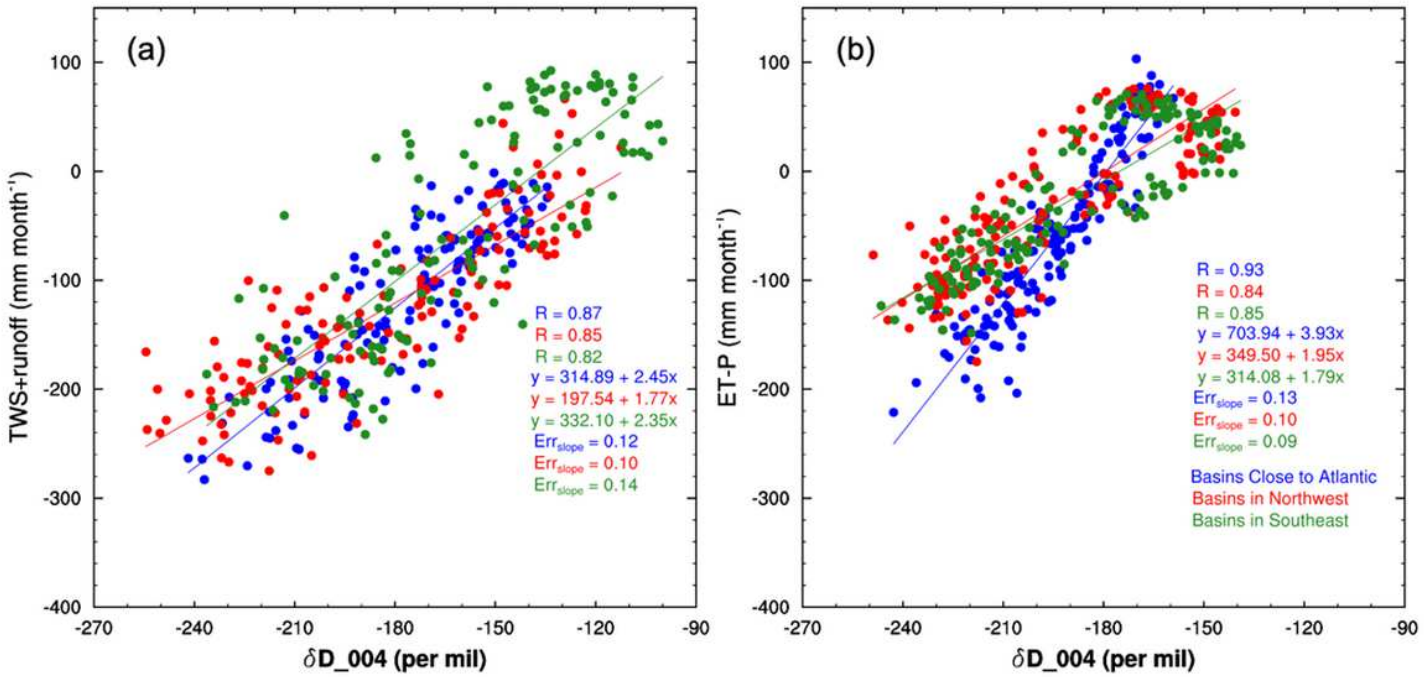

Figure 3

(a) Regressions of TWS/discharge estimated ET-P on AIRS δD_004 and (b) regressions of ET-P on δD_004 in ICAM. Basins close to the Atlantic are Basins 1, 3, 10, and 12; basins in the Northwest are basins 5, 8, 9,13, and 14; the rest of the basins are in the Southeast. Here, the basins close to the Atlantic have a higher slope than the others, according to both the observations and model, indicating a different moisture source.

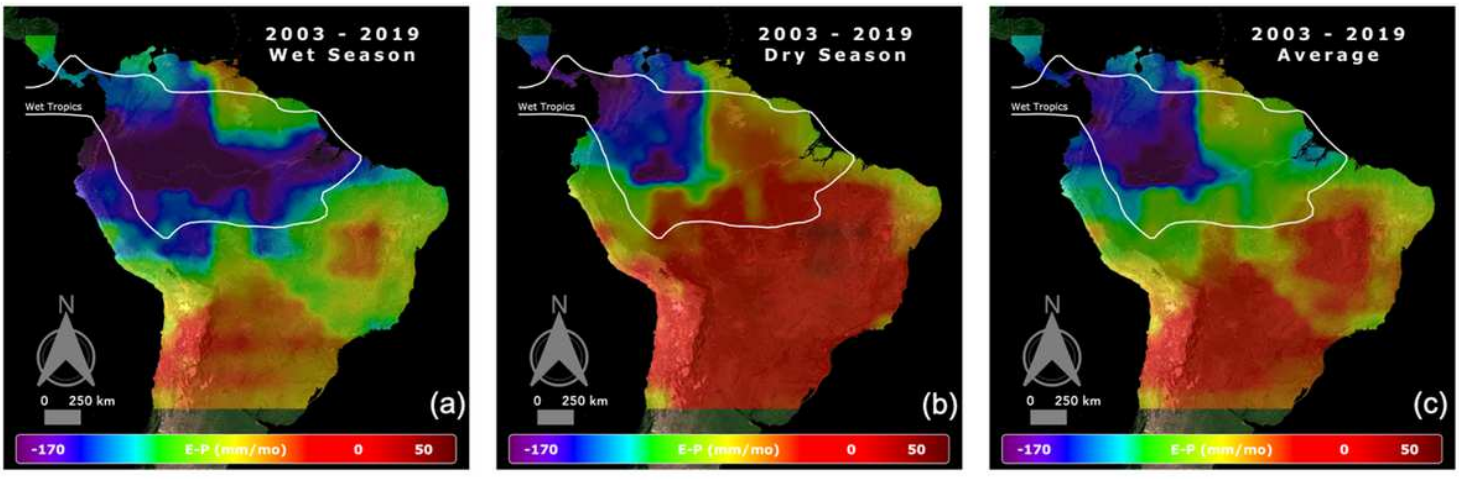

Figure 4

ET-P derived from δD_004 for the wet season (Jan-Jun), the dry season (Jul-Dec), and the annual average. The solid white line indicates the approximate boundary of the wet tropics, with rainfall inside the white line exceeding 160 mm month-1 on average over the year.

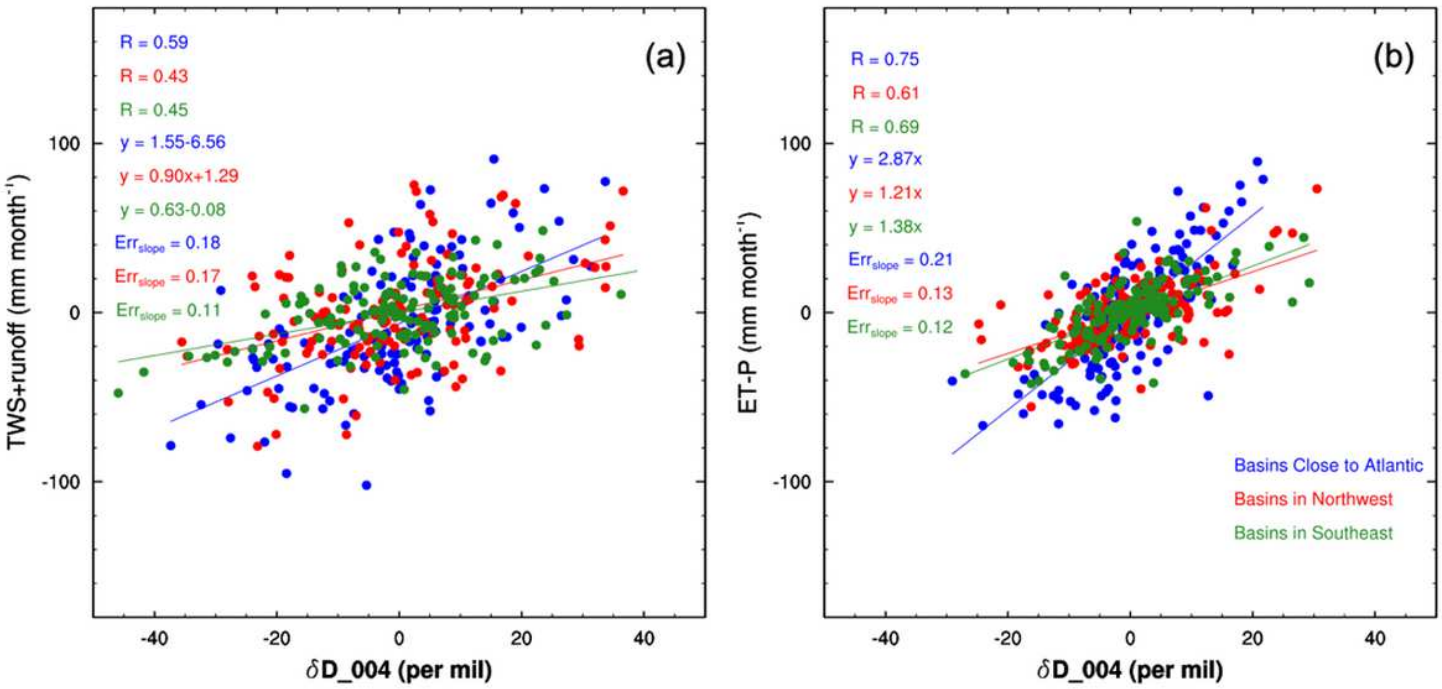

Figure 5

Similar to Figure 3, this figure shows IAV (a) regressions of TWS/discharge estimated ET-P on AIRS δD_004 and (b) regressions of ET-P on δD_004 in iCAM. Here, all the time series from observations and the model are de-seasonalized.

Supplementary Files

This is a list of supplementary files associated with this preprint. Click to download.

- ShiWordenAmazonWaterSupplementary08022021.docx